Journal of Innovative Technology, Vol. 7, No. 1, pp. 117-124, March 2025
http://doi.org/10.29424/JIT.202503_7(1).0009

Mountain Gazelle optimization algorithm for identification of nonlinear Hammerstein output error systems

Muhammad Aown Ali [1], Naveed Ishtiaq Chaudhary [2*], Chien-Chou Lin [3], Wei-Lung Mao [4]

ABSTRACT

This study provides an inclusive review of the vigorous identification of the Hammerstein-output error system (HOES). The mean-square-error-based fitness function is used to explore the efficacy of the mountain gazelle optimization algorithm (MGO). The auxiliary-model with the key-term separation principle is combined to approximate the parameters for accurately identifying complex parameters of the system. The efficacy of the nature-inspired heuristic optimization algorithm i.e., the mountain gazelle optimization algorithm is exploited for the Hammerstein-output error system (HOES) and is evaluated through accuracy, convergence speed, and estimation of actual parameters as compared with three states of the art algorithms that are whale-optimization algorithm (WOA), grey-wolf optimization algorithm (GWO), and arithmetic-optimization algorithm (AO).

Keywords: Nonlinear systems; Hammerstein-output error model; System identification; Optimization technique; Mountain gazelle algorithm.

1. INTRODUCTION

Nonlinear systems are complex [1-2] because their behavior doesn't follow a straight line, making them harder to predict. The systems can show unexpected patterns, which are similar to real-world processes. The Hammerstein structure is a type of nonlinear system that is commonly used in many systems [3-4], signal processing [5-6], and system identification [7-8]. These models consist of two parts a static block of nonlinear systems [9-10] and a dynamic block of linear systems [11-12]. Nonlinear Hammerstein structures are widely used in different applications such as turntable servo systems [13-14], aeroelastic systems [15-16], and recurrent neural networks [17-18]. Identifications of nonlinear systems are difficult due to their unpredictable behavior and sensitivity to initial conditions. It holds a very important role in many fields such as intelligent computing [19-20], machine learning [21-22], artificial intelligence [23], deep learning [24], fluid mechanics [25], structural systems [26], and health monitoring systems [27-30]. On the whole, the Hammerstein structures [31-32] can discriminate between nonlinearities and linear dynamics thus making it a multipurpose tool for modeling complicated systems in various fields as discussed. It provides insights that aid in the control, optimization, and prediction of systems. In optimization and search algorithms, there are primarily two types of approaches; global search algorithms [33] and local search algorithms [34]. Local search algorithms aim to focus on improving a single solution by iterating and moving to neighboring solutions, often leading to faster convergence but potentially getting trapped in local optima. Some of the local search optimization algorithms are as follows least mean square algorithm [35], fractional gradient algorithm [36], and local beam search algorithm [37], etc. On the other hand, global search algorithms aim to explore the entire solution space to find the global optimum, overcoming the risk of getting stuck in local optima. Some of the global search algorithms are as follows particle swarm optimization [38], genetic algorithm [39], cuckoo-search algorithm [40], improved-shuffled frog leaping algorithm [41], etc. mountain gazelle optimization algorithm [42] is also considered a global search algorithm. It is a heuristic technique inspired by the behavior of gazelles in nature especially their way of balancing exploration and exploitation while searching for food or shelter in mountain terrains. The algorithm aims to explore the solution space broadly to find global optima.

The novel insights of the study are as follows:

- The Mountain Gazelle optimization algorithm (MGO) is exploited for the identification of the Hammerstein-output error system.
- The fitness function constructed on the error of the mean square is premeditated to minimize the gap between the predictable response and the real response of the HOE system.
- An auxiliary-model along with key term separation is applied to manage the indeterminable terms and simplify cross-product terms in the HOES model.
- The efficiency of the mountain gazelle optimization algorithm is recognized concerning the precision of predictable parameters, converging rapidity, and consistency in assessment with different state-of-the-art algorithms.

The graphical representation of the study is depicted in Figure 1. The model structure of Hammerstein-output error is described in section 2. The methodology that defines the algorithm and its

Manuscript received November 29, 2024; revised December 26, 2024; accepted January 2, 2025.

[1] Master Student, Department of Computer Science and Information Engineering, National Yunlin University of Science and Technology, Taiwan, R.O.C.

[2*] Assistant Professor (corresponding author), Future Technology Research Center, National Yunlin University of Science and Technology, Taiwan, R.O.C. (email: chaudni@yuntech.edu.tw)

[3] Professor, Department of Computer Science and Information Engineering, National Yunlin University of Science and Technology, Taiwan, R.O.C.

[4] Professor, Department of Electrical Engineering, National Yunlin University of Science and Technology, Taiwan, R.O.C.

working is described in section 3 and the analysis of the study and conclusion are described in section 4 and section 5 respectively.

2. HAMMERSTEIN-OUTPUT ERROR SYSTEM (HOES)

The Hammerstein-output error system (HOES) [43] model is shown in Figure 2 and mathematically described in Equation (1)

$$A(\mathrm{x}) = \frac{M(e)}{B(e)}\bar{\mathrm{f}}(\mathrm{x}) + \phi(\mathrm{x}), \tag{1}$$

where, $A(x)$ denotes the result of the system, $\frac{M(e)}{B(e)}$ denotes the operators of the polynomial shift, $\bar{\mathrm{f}}(\mathrm{x})$ denotes the nonlinear result and $\phi(\mathrm{x})$represents the noise. The operators of the polynomial shift are represented in Equations (2) and (3)

$$B(e) = 1 + b_1 e^{-1} + b_2 e^{-2} + \cdots + b_{\mathrm{n}_b} e^{-\mathrm{n}_b}, \tag{2}$$

$$M(e) = m_0 + m_1 e^{-1} + m_2 e^{-2} + \cdots + m_{\mathrm{n}_m} e^{-\mathrm{n}_m}. \tag{3}$$

The noise free part of the HOES model is shown in Equation (4)

$$\beta(\mathrm{x}) = \frac{M(e)}{B(e)}\bar{\mathrm{f}}(\mathrm{x}), \tag{4}$$

as mentioned in Equation (4), the result of the nonlinear part as a key term [44] can be expressed in Equation (5) and Equation (6)

$$\beta(\mathrm{x}) = -\sum_{\mathrm{k}=1}^{\mathrm{n}_b} b_k \beta(\mathrm{x}-\mathrm{k}) + \sum_{\mathrm{k}=1}^{\mathrm{n}_m} m_k \bar{\mathrm{f}}(\mathrm{x}-\mathrm{k}) + m_0\,\bar{\mathrm{f}}(\mathrm{x}), \tag{5}$$

$$\beta(\mathrm{x}) = -\sum_{\mathrm{k}=1}^{\mathrm{n}_b} b_k \beta(\mathrm{x}-\mathrm{k}) + \sum_{\mathrm{k}=1}^{\mathrm{n}_m} m_k \bar{\mathrm{f}}(\mathrm{x}-\mathrm{k}) + \sum_{\mathrm{i}=1}^{z} z_i R_i\,(\mathrm{f}(\mathrm{x})), \tag{6}$$

so, the above-shown variables are the vector parameters shown below in Equation (7), Equation (8), and Equation (9)

$$\mathbf{b} = \left[b_1, b_2, \ldots, b_{\mathrm{n}_b}\right]^{\mathrm{T}}, \tag{7}$$

$$\mathbf{m} = \left[m_1, m_2, \ldots, m_{\mathrm{n}_m}\right]^{\mathrm{T}}, \tag{8}$$

$$\mathbf{m} = \left[m_1, m_2, \ldots, m_{\mathrm{n}_m}\right]^{\mathrm{T}}, \tag{9}$$

The mathematical expressions of the data vectors are shown in Equations (10), (11), and (12)

$$\boldsymbol{\theta}_{\boldsymbol{b}}(\mathbf{x}) = [-\beta(\mathrm{x}-1), -\beta(\mathrm{x}-2), \ldots, -\beta(\mathrm{x}-\mathrm{n}_b)]^{\mathrm{T}}, \tag{10}$$

$$\boldsymbol{\theta}_{\boldsymbol{m}}(\mathbf{x}) = \left[\bar{\mathrm{f}}(\mathrm{x}-1), \bar{\mathrm{f}}(\mathrm{x}-2), \ldots, \bar{\mathrm{f}}(\mathrm{x}-\mathrm{n}_m)\right]^{\mathrm{T}}, \tag{11}$$

$$\boldsymbol{R}(\mathbf{x}) = [R_1(\mathrm{f}(\mathrm{x})), R_2(\mathrm{f}(\mathrm{x})), \ldots, R_z(\mathrm{f}(\mathrm{x}))]^{\mathrm{T}}, \tag{12}$$

Equations (13), (14), and (15) derive the mathematical expressions mentioned in Equation (4) to calculate it.

$$\bar{\mathrm{f}}(\mathrm{x}) = \boldsymbol{R}^{\mathbf{T}}(\mathrm{x})z, \tag{13}$$

$$\beta(\mathrm{x}) = \boldsymbol{\theta}_{\boldsymbol{b}}^{\mathbf{T}}(\mathrm{x})\mathrm{b} + \boldsymbol{\theta}_{\boldsymbol{m}}^{\mathbf{T}}(\mathrm{x})\mathrm{m} + \boldsymbol{R}^{\mathbf{T}}(\mathrm{x})z, \tag{14}$$

$$H(\mathrm{x}) = \boldsymbol{\theta}_{\boldsymbol{b}}^{\mathbf{T}}(\mathrm{x})\mathrm{b} + \boldsymbol{\theta}_{\boldsymbol{b}}^{\mathbf{T}}(\mathrm{x})\mathrm{m} + \boldsymbol{R}^{\mathbf{T}}(\mathrm{x})\mathrm{z} + \phi(\mathrm{x}). \tag{15}$$

The parameter and information vector are represented in Equations (16) and (17)

$$\mathbf{pa} = [\boldsymbol{b}^{\mathbf{T}}, \boldsymbol{m}^{\mathbf{T}}, \boldsymbol{z}^{\mathbf{T}}]^{\mathbf{T}}, \tag{16}$$

$$\boldsymbol{v}(\mathbf{t}) = \left[\boldsymbol{\theta}_{\boldsymbol{b}}^{\mathbf{T}}(\mathrm{x}), \boldsymbol{\theta}_{\boldsymbol{m}}^{\mathbf{T}}(\mathrm{x}), \boldsymbol{R}^{\mathbf{T}}(\mathrm{x})\right]^{\mathbf{T}}, \tag{17}$$

by adding Equation (16) and (17) in (15), the resultant equation shown in (18)

$$H(\mathrm{x}) = \boldsymbol{v}^{\mathbf{T}}(\mathrm{x})\mathbf{pa} + \phi(\mathrm{x}). \tag{18}$$

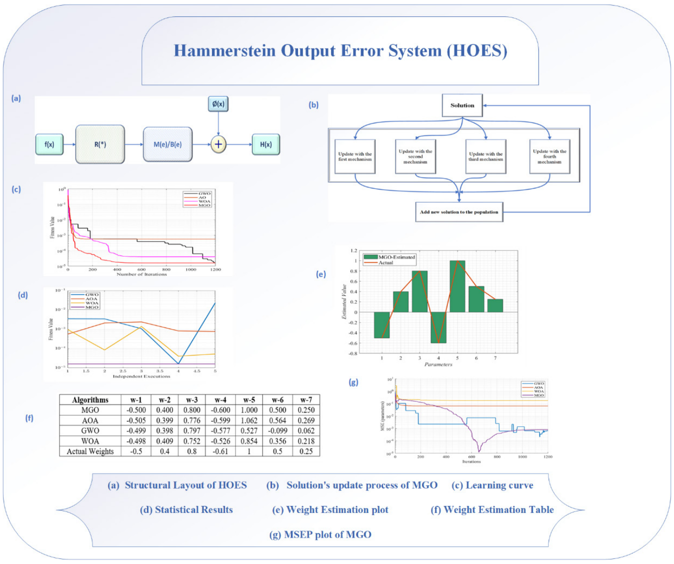

Fig. 1 Graphical depiction of the study

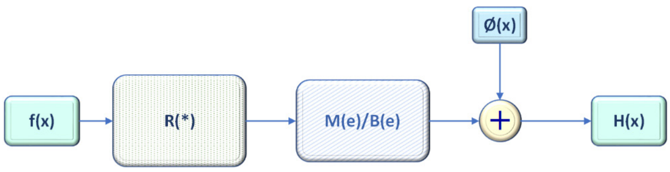

Fig. 2 HOES model layout

3. The mountain gazelle optimization algorithm (MGO)

A hierarchy of mountain wild gazelles and social structure inspires the nature-inspired mountain gazelle optimization algorithm. its mathematical model is derived in the following section [42].

3.1 Mathematical Model of the Algorithm

The social behavior and life patterns of the mountain gazelle inspire the mountain gazelle optimization algorithm (MGO). It made optimization through four key dynamics: bachelor male herds, maternity herds, solitary territorial males, and food migration. Each gazelle represents a solution that is preserved weak ones are discarded and new solutions arise from existing herds. The best global solution represents a dominant adult male gazelle in the territory. This process is mathematically formulated to simulate the optimization process [42]. Figure 3 shows how the exploitation and exploitation phases perform simultaneously, enabling solutions to move forward towards the best while exploring through four defined mechanisms.

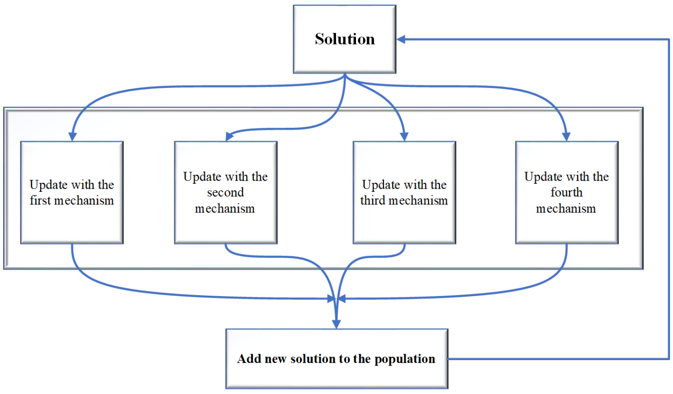

Fig. 3 Solution's update process of MGO

Equation (19) models the territorial behavior and defense behavior () of adult male mountain gazelles as depicted in [42].

$$TESOM = M_{gazelle} - \left|(jt_1 \times BH - jt_2 \times Y(x)) \times C\right| \times Fof_j. \quad (19)$$

Equation (20) represents the behavioral interactions within materiality herds (), including the birth of male gazelles

$$MAHE = (MW + Fof_{1,j}) + (jt_3 \times M_{gazelle} - jt_4 \times Y_{rnd} \times Fof_{1,j}. \quad (20)$$

Equation (21) shows the territorial battles and competition for females among male gazelles (*BAMH*).

$$BAMH = (Y(x) - R) + (jt_5 \times M_{gazelle} - jt_6 \times MW) \times Fof_{1,j}. \quad (21)$$

Equation (22) models the foraging and migratory behavior of mountain gazelles (*MTSFF*).

$$MTSFF = (UOB - LOB) \times j_7 + LOB, \quad (22)$$

where UOB and LOB are the upper and lower bounds. These upper described four mechanisms generate new gazelle populations with each generation representing one replication. High-quality gazelles are retained while weaker ones are removed with the best gazelle symbolizing the adult male holding territory [42].

4. RESULTS AND DISCUSSIONS

The outcome of the imitations for the finding of the Hammerstein-output error system (HOES) with the mountain gazelle optimization algorithm (MGO) is shown in this portion. The efficacy of the mountain gazelle optimization algorithm (MGO) is validated in noise-less and noise-full conditions i.e., ϕ=0, 0.005, 0.0005, and 0.0005. The imitations are performed for the iteration's level of 1200 with a population size of 200. The efficacy is analyzed through learning curves, statistical analysis, fitness values, and comparison with some other algorithms' performance compared with our proposed algorithms. The results are shown in tables and graphical form. The parameters of the mountain gazelle optimization algorithm (MGO) are taken from [43] while the parameters of the whale optimization algorithm (WOA), grey wolf optimization algorithm (GWO), and arithmetic optimization algorithm (AO) are taken from [45]-[47]. The imitations are run in MATLAB, core i-5 12th generation system.

4.1 Numerical example of Hammerstein-output error system (HOES)

The system weights parameters of the Hammerstein-output error system (HOES) are taken from [48]. Figure 4 shows the converging curves of our algorithm along with its state-of-the-art algorithms showing that our proposed MGO performing well as compared to their state-of-the-art algorithm. Figure 5 shows the statistical analysis presenting that the MGO is consistent, stable, and gives non-fluctuating results as compared to other algorithms, and Table 1-4 Shows the best fitness (BF), worst fitness (WF), standard deviation (STD), and average fitness (AF) values of all the algorithms showing the efficacy and robustness of the MGO. From the figure and tables, it is witnessed that the MGO performs well in all the noise scenarios i.e., ϕ=0, 0.005, 0.0005, and 0.0005 in terms of accuracy, robustness, accuracy, and achieving higher fitness value.

Table 1 Best fitness, Average fitness, STD, and Worst-fitness of all counterparts for ϕ=0

Algorithms	BF	AF	STD	WF
MGO	9.9045E-16	6.8341E-13	8.7422E-13	2.0168E-12
AOA	4.3287E-05	4.0727E-03	3.9756E-03	9.9278E-03
GWO	1.1659E-03	5.5810E-03	5.9856E-03	1.5689E-02
WOA	3.5811E-04	3.7039E-03	3.3637E-03	7.6082E-03

Table 2 Best fitness, Average fitness, STD, and Worst-fitness of all counterparts for ϕ=0.005

Algorithms	BF	AF	STD	WF
MGO	1.5945E-05	1.5945E-05	3.0023E-11	1.5945E-05
AOA	5.5888E-04	1.3288E-03	8.5334E-04	2.3910E-03
GWO	1.6054E-05	6.2923E-03	9.7054E-03	2.3442E-02
WOA	4.0242E-05	5.0465E-04	6.2802E-04	1.3824E-03

Table 3 Best fitness, Average fitness, STD, and Worst-fitness of all counterparts for ϕ=0.0005

Algorithms	BF	AF	STD	WF
MGO	1.2931E-07	1.2931E-07	8.3850E-19	1.2931E-07
AOA	3.7757E-04	4.4497E-02	9.7904E-02	2.1963E-01
GWO	1.6232E-07	3.2725E-02	6.7279E-02	1.5290E-01
WOA	3.1326E-04	1.0359E-03	4.7936E-04	1.5363E-03

Table 4 Best fitness, Average fitness, STD, and Worst-fitness of all counterparts for ϕ=0.00005

Algorithms	BF	AF	STD	WF
MGO	2.6114E-09	2.6114E-09	1.6112E-19	2.6114E-09
AOA	9.0910E-05	1.3025E-03	1.9270E-03	4.7148E-03
GWO	4.5647E-04	2.4002E-03	3.4602E-03	8.5742E-03
WOA	3.4733E-05	3.7979E-04	3.1235E-04	7.6373E-04

ϕ = 0

ϕ = 0.005

ϕ = 0.0005

ϕ = 0.00005

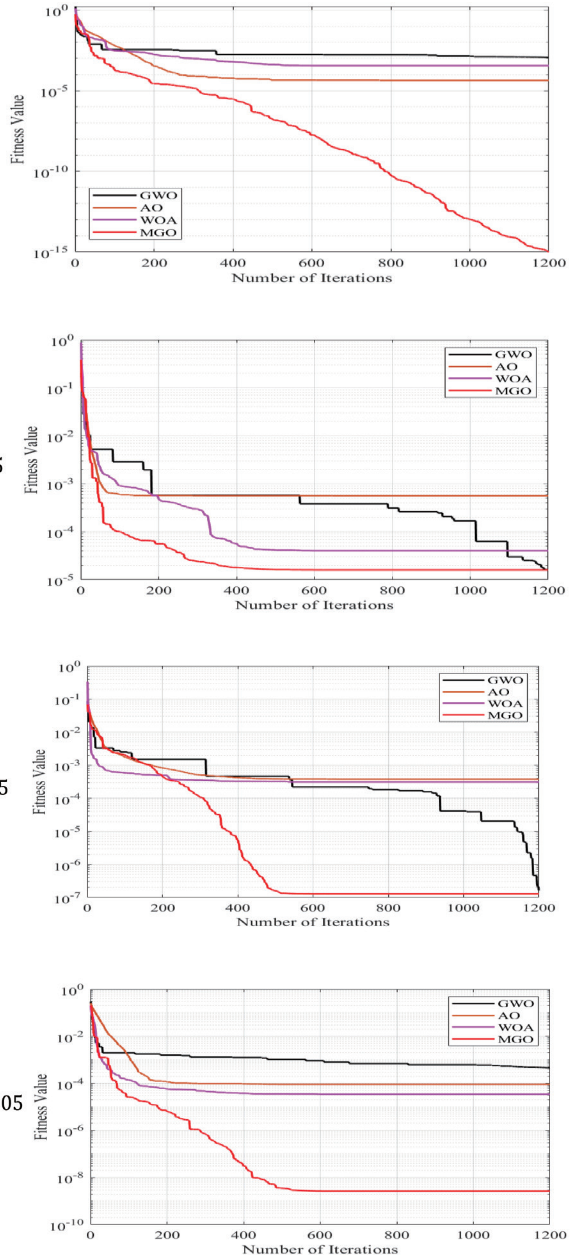

Fig. 4 Converging curves of our algorithm along with its state-of-the-art algorithms

ϕ = 0

ϕ = 0.005

ϕ = 0.0005

ϕ = 0.00005

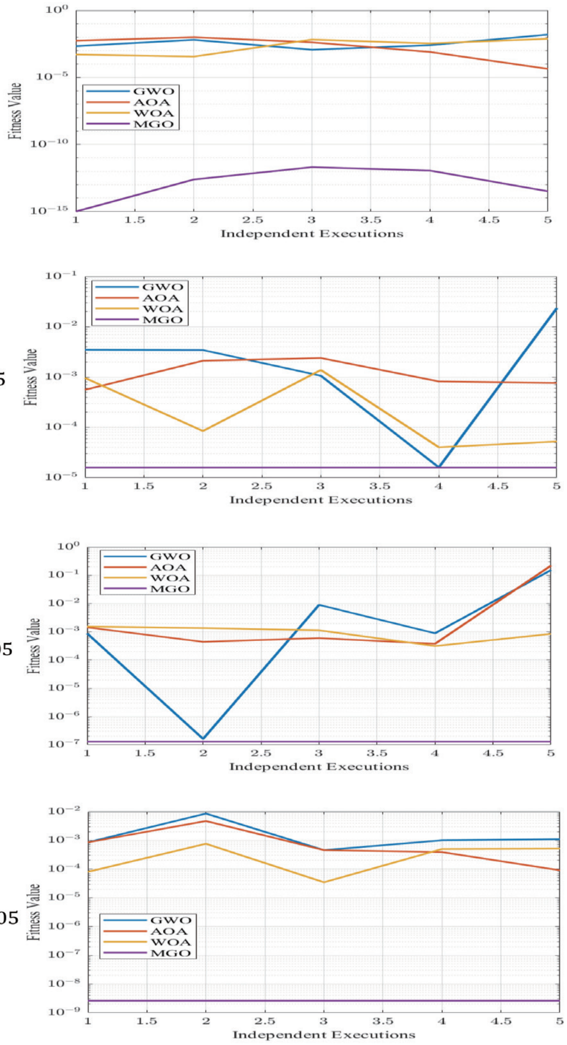

Fig. 5 Statistical analysis of our algorithm along with its state-of-the-art algorithms

To additionally inspect the efficacy of the MGO in terms of weight approximation, it is witnessed from Figure 6 and Table 5-8 that the MGO predicts the correct parameters effectively in all noise conditions i.e., ϕ=0, 0.005, 0.0005, and 0.0005 consistently. Hence growing the noise affects the performance of the MGAO but still, it shows a high level of performance as compared to its

ϕ = 0

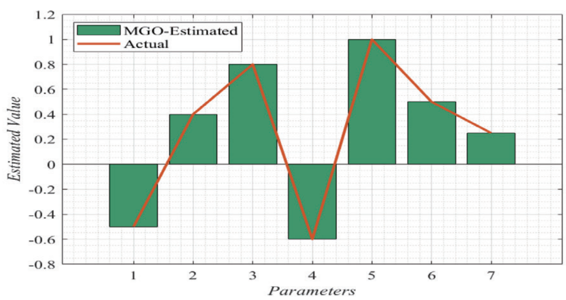

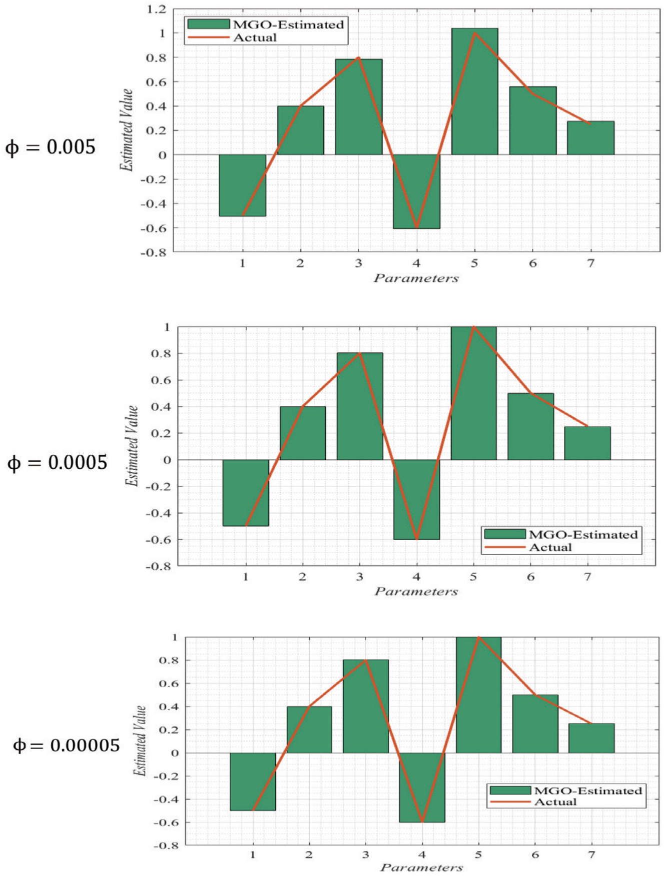

Fig. 6 Weight approximation of our algorithm along with its state-of-the-art algorithms

Table 5 Weight approximation of all counterparts for ϕ=0

Algorithms	W1	W2	W3	W4	W5	W6	W7
MGO	-0.500	0.400	0.800	-0.600	1.000	0.500	0.250
AOA	-0.505	0.399	0.776	-0.599	1.062	0.564	0.269
GWO	-0.499	0.398	0.797	-0.577	0.527	-0.099	0.062
WOA	-0.498	0.409	0.752	-0.526	0.854	0.356	0.218
Actual Weights	-0.5	0.4	0.8	-0.61	1	0.5	0.25

Table 6 Weight approximation of all counterparts for ϕ=0.005

Algorithms	W1	W2	W3	W4	W5	W6	W7
MGO	-0.506	0.399	0.786	-0.607	1.039	0.558	0.274
AOA	-0.486	0.400	0.825	-0.570	0.632	-0.030	0.056
GWO	-0.506	0.399	0.787	-0.606	1.034	0.551	0.272
WOA	-0.511	0.405	0.764	-0.588	1.028	0.540	0.269
Actual Weights	-0.5	0.4	0.8	-0.61	1	0.5	0.25

Table 7 Weight approximation of all counterparts for ϕ=0.0005

Algorithms	W1	W2	W3	W4	W5	W6	W7
MGO	-0.506	0.399	0.786	-0.607	1.039	0.558	0.274
AOA	-0.486	0.400	0.825	-0.570	0.632	-0.030	0.056
GWO	-0.506	0.399	0.787	-0.606	1.034	0.551	0.272
WOA	-0.511	0.405	0.764	-0.588	1.028	0.540	0.269
Actual Weights	-0.5	0.4	0.8	-0.61	1	0.5	0.25

Table 8 Weight approximation of all counterparts for ϕ=0.00005

Algorithms	W1	W2	W3	W4	W5	W6	W7
MGO	-0.500	0.400	0.800	-0.600	1.000	0.500	0.250
AOA	-0.499	0.403	0.813	-0.617	1.098	0.672	0.324
GWO	-0.493	0.398	0.809	-0.570	0.778	0.101	0.069
WOA	-0.499	0.402	0.798	-0.589	0.948	0.398	0.201
Actual Weights	-0.5	0.4	0.8	-0.61	1	0.5	0.25

The efficacy and robustness of MGO are also analyzed in terms of parameters mean square error of third-order nonlinear HOES that is calculated through predicted and calculated parameters in all noise scenarios i.e., ϕ=0, 0.005, 0.0005, and 0.0005 as shown in Figure 7. It is clear from the graphs that MGO performs well in all noise scenarios.

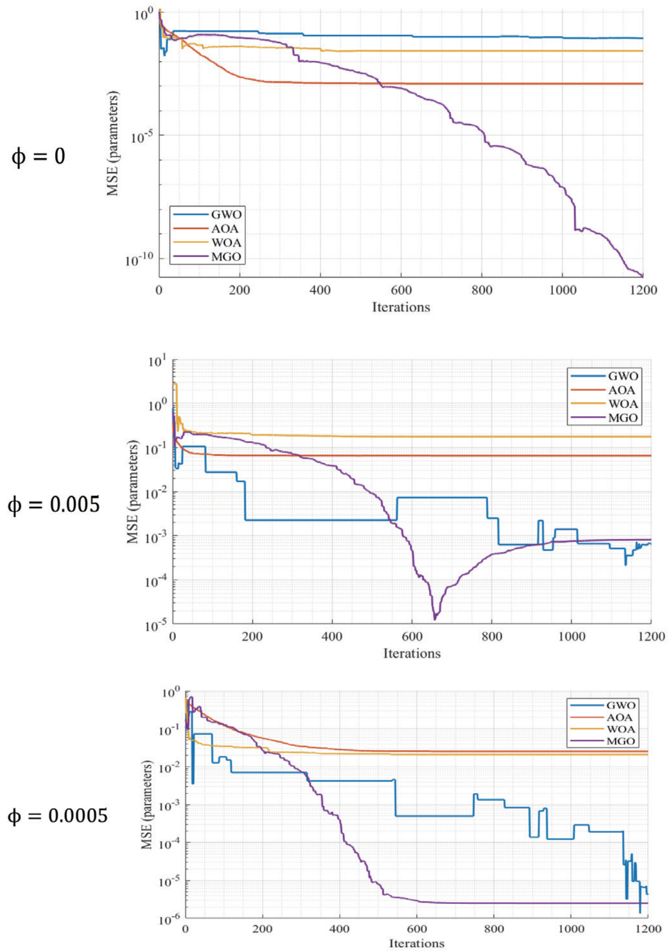

$\phi = 0.00005$

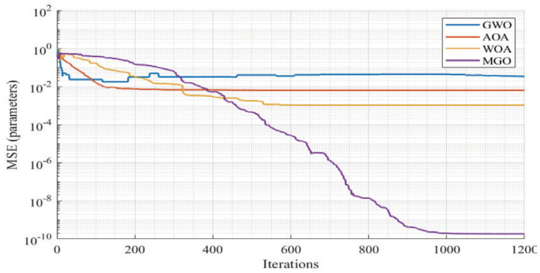

Fig. 7 The mean square error plot of our algorithm along with its state-of-the-art algorithms

5. CONCLUSION

In this study, the mountain gazelle optimization algorithm (MGO) is exploited for the parameter estimation of the Hammerstein-output error system, an auxiliary model structure with the key-term principle and the finding concludes that the MGO is performing well and giving promising outcomes in terms of fitness values, consistent behavior, non-fluctuating outcomes, and estimation of original weights of the system showing its robustness and efficacy. The simulation is run on 5 independent runs with a population size of 200 on 1200 iterations on different noise levels i.e., and gave the fitness values of 9.9045E-16, 1.5945E-05, 1.2931E-07, 2.6114E-09. Future work will explore the performance of MGO for more complex systems such as Fractional Hammerstein-output error systems or for more complex nonlinearities such as geometric nonlinearity, material nonlinearity, contact nonlinearity, boundary nonlinearity, etc.

REFERENCES

[1] Wei, F., Zhang, L., Niu, B., & Zong, G. (2024). "Adaptive decentralized fixed-time neural control for constrained strong interconnected nonlinear systems with input quantization." *International Journal of Robust and Nonlinear Control*, **34**(14), 9899-9927.

[2] Khan, T. A., Chaudhary, N. I., Khan, Z. A., Mehmood, K., Hsu, C. C., & Raja, M. A. Z. (2024). "Design of Runge-Kutta optimization for fractional input nonlinear autoregressive exogenous system identification with key-term separation. Chaos," *Solitons & Fractals,* **182**, 114723.

[3] Javed, M. U., Javaid, N., Alrajeh, N., Shafiq, M., & Choi, J. G. (2024). "Mutual authentication enabled trust model for vehicular energy networks using Blockchain in Smart Healthcare Systems." *Simulation Modelling Practice and Theory,* **136**, 103006.

[4] Jamal, A., Javed, M. U., Alrajeh, N., Bouk, S. H., & Javaid, N. (2024). "Blockchain based reputation management, data storage and distributed revocation in vehicular energy networks in smart health care systems." *Cluster Computing,* **27**(2), 2151-2163.

[5] Li, F., Jia, L., & Gu, Y. (2023). "Identification of nonlinear process described by neural fuzzy Hammerstein-Wiener model using multi-signal processing." *Advances in Manufacturing,* **11**(4), 694-707.

[6] Zhu, X., Li, F., Li, C., Jia, L., & Cao, Q. (2021, May). "Parameter estimation of the Hammerstein output error model using multi-signal processing." *In 2021 IEEE 10th Data Driven Control and Learning Systems Conference (DDCLS)* (pp. 1285-1290). IEEE.

[7] Mehmood, K., Chaudhary, N. I., Khan, Z. A., Cheema, K. M., Raja, M. A. Z., Milyani, A. H., & Azhari, A. A. (2022). "Nonlinear hammerstein system identification: A novel application of marine predator optimization using the key term separation technique." *Mathematics,* **10**(22), 4217.

[8] Ali, M. A., Chaudhary, N. I., Khan, T. A., Mao, W. L., Lin, C. C., & Raja, M. A. Z. (2024). "Design of key term separated identification model for fractional input nonlinear output error systems: Auxiliary model based Runge Kutta optimization algorithm." *Chaos, Solitons & Fractals,* **189**, 115696.

[9] Schoukens, M., & Tiels, K. (2017). "Identification of block-oriented nonlinear systems starting from linear approximations: A survey." *Automatica,* **85**, 272-292.

[10] Van Mulders, A., Schoukens, J., & Vanbeylen, L. (2013). "Identification of systems with localised nonlinearity: From state-space to block-structured models." *Automatica,* **49**(5), 1392-1396.

[11] da Cunha, R. D., & Becker, D. (2007). "Dynamic block GMRES: an iterative method for block linear systems." *Advances in Computational Mathematics,* **27**(4), 423-448.

[12] Zhuang, Z., Tao, H., Chen, Y., Stojanovic, V., & Paszke, W. (2022). "An optimal iterative learning control approach for linear systems with nonuniform trial lengths under input constraints." *IEEE Transactions on Systems, Man, and Cybernetics: Systems,* **53**(6), 3461-3473.

[13] Li, L., Zhang, H., & Ren, X. (2020). "A modified multi-innovation algorithm to turntable servo system identification." *Circuits, Systems, and Signal Processing,* **39**, 4339-4353.

[14] Zhang, Q., Wang, Q., & Li, G. (2016). "Nonlinear modeling and predictive functional control of Hammerstein system with application to the turntable servo system." *Mechanical Systems and Signal Processing,* **72**, 383-394.

[15] Zeng, J., Baldelli, D. H., & Brenner, M. (2008). "Novel nonlinear Hammerstein model identification: Application to nonlinear aeroelastic/aeroaervoelastic system." *Journal of guidance, control, and dynamics,* **31**(6), 1677-1686.

[16] Yao, X., Huang, R., & Hu, H. (2023). "Enhanced nonlinear state–space identification for efficient transonic aeroelastic predictions." *Journal of Fluids and Structures,* **11**6, 103792.

[17] Chen, Y. C., Lei, T. C., Yao, S., & Wang, H. P. (2020). "PM2. 5 prediction model based on combinational hammerstein recurrent neural networks." *mathematics,* **8**(12), 2178.

[18] Abouda, S. E., Abid, D. B. H., Elloumi, M., Koubaa, Y., & Chaari, A. (2020). "Identification of non-linear stochastic systems using a new Hammerstein-Wiener neural network: a simulation study through a non-linear hydraulic process." *International Journal of Computer Applications in Technology,* **63**(3), 241-256.

[19] Madkour, A. A. M., Hossain, M. A., Dahal, K. P., & Yu, H. (2004). Real-time system identification using intelligent algo-

rithms.

[20] Zhu, S., Yu, T., Xu, T., Chen, H., Dustdar, S., Gigan, S., ... & Pan, Y. (2023). "Intelligent computing: the latest advances, challenges, and future." *Intelligent Computing,* **2**, 0006.

[21] Chiuso, A., & Pillonetto, G. (2019). "System identification: A machine learning perspective." *Annual Review of Control, Robotics, and Autonomous Systems,* **2**(1), 281-304.

[22] Pillonetto, G., Dinuzzo, F., Chen, T., De Nicolao, G., & Ljung, L. (2014). "Kernel methods in system identification, machine learning and function estimation: A survey." *Automatica,* **50**(3), 657-682.

[23] Savulescu, C., & Polkowski, Z. (2017, June). "An approach for systems identification using artificial inteligence." *In 2017 9th international conference on Electronics, Computers and Artificial Intelligence (ECAI)* (pp. 1-4). IEEE.

[24] De la Rosa, E., & Yu, W. (2016). "Randomized algorithms for nonlinear system identification with deep learning modification." *Information Sciences*, **36**4, 197-212.

[25] Liu, X., Jiang, J. Z., Titurus, B., & Harrison, A. (2018). "Model identification methodology for fluid-based inerters." *Mechanical Systems and Signal Processing*, **106**, 479-494.

[26] Ding, F., Xu, L., Zhang, X., Zhou, Y., & Luan, X. (2024). "Recursive identification methods for general stochastic systems with colored noises by using the hierarchical identification principle and the filtering identification idea." *Annual Reviews in Control,* **57**, 100942.

[27] Yan, W. J., Zhao, M. Y., Sun, Q., & Ren, W. X. (2019). "Transmissibility-based system identification for structural health Monitoring: Fundamentals, approaches, and applications." *Mechanical Systems and Signal Processing*, **117**, 453-482.

[28] Wu, R. T., & Jahanshahi, M. R. (2020). "Data fusion approaches for structural health monitoring and system identification: Past, present, and future." *Structural Health Monitoring,* **19**(2), 552-586.

[29] Reynders, E., Wursten, G., & De Roeck, G. (2014). "Output-only structural health monitoring in changing environmental conditions by means of nonlinear system identification." *Structural Health Monitoring*, **13**(1), 82-93.

[30] Chen, H., Kurt, M., Lee, Y. S., McFarland, D. M., Bergman, L. A., & Vakakis, A. F. (2014). "Experimental system identification of the dynamics of a vibro-impact beam with a view towards structural health monitoring and damage detection. " *Mechanical Systems and Signal Processing,* **46**(1), 91-113.

[31] Mehmood, A., Raja, M. A. Z., Shi, P., & Chaudhary, N. I. (2022). "Weighted differential evolution-based heuristic computing for identification of Hammerstein systems in electrically stimulated muscle modeling." *Soft Computing,* **26**(17), 8929-8945.

[32] Malik, M. F., Chang, C. L., Aslam, M. S., Chaudhary, N. I., & Raja, M. A. Z. (2022). "Fuzzy-evolution computing paradigm for fractional Hammerstein control autoregressive systems." *International Journal of Fuzzy Systems,* **24**(5), 2447-2475.

[33] Javaid, N., Javaid, S., Abdul, W., Ahmed, I., Almogren, A., Alamri, A., & Niaz, I. A. (2017). "A hybrid genetic wind driven heuristic optimization algorithm for demand side management in smart grid." *Energies,* **10**(3), 319.

[34] Rahim, S., Javaid, N., Ahmad, A., Khan, S. A., Khan, Z. A., Alrajeh, N., & Qasim, U. (2016). "Exploiting heuristic algorithms to efficiently utilize energy management controllers with renewable energy sources." *Energy and Buildings,* **129**, 452-470.

[35] Chaudhary, N. I., Ahmed, M., Dedovic, N., & Raja, M. A. Z. (2020). "Momentum least mean square paradigm for the measurement of nonlinear CARAR system parameters." *Journal of Computational and Nonlinear Dynamics,* **15**(3), 031004.

[36] Chaudhary, N. I., Khan, Z. A., Kiani, A. K., Raja, M. A. Z., Chaudhary, I. I., & Pinto, C. M. (2022). "Design of auxiliary model based normalized fractional gradient algorithm for nonlinear output-error systems." *Chaos, Solitons & Fractals,* **163**, 112611.

[37] Shetty, A., Kale, Y., Patil, Y., Patil, R., & Sharma, S. (2024). "Optimal transformers based image captioning using beam search." *Multimedia Tools and Applications,* **83**(16), 47963-47977.

[38] Yin, L., & Zhang, Y. (2024). "Particle swarm optimization based on data driven for EV charging station siting." *Energy,* **310**, 133197.

[39] Alhijawi, B., & Awajan, A. (2024). "Genetic algorithms: Theory, genetic operators, solutions, and applications." *Evolutionary Intelligence,* **17**(3), 1245-1256.

[40] Yaqoob, A., Verma, N. K., & Aziz, R. M. (2024). "Optimizing gene selection and cancer classification with hybrid sine cosine and cuckoo search algorithm." *Journal of Medical Systems,* **48**(1), 10.

[41] Mehta, S. (2024). "Improved shuffled frog leaping algorithm with unsupervised population partitioning strategies for complex optimization problems." *Journal of Combinatorial Optimization,* **47**(2), 6.

[42] Abdollahzadeh, B., Gharehchopogh, F. S., Khodadadi, N., & Mirjalili, S. (2022). "Mountain gazelle optimizer: a new nature-inspired metaheuristic algorithm for global optimization problems." *Advances in Engineering Software,* **174**, 103282.

[43] Ding, F., Shi, Y., & Chen, T. (2007). "Auxiliary model-based least-squares identification methods for Hammerstein output-error systems." *Systems & Control Letters,* **56**(5), 373-380.

[44] Shen, Q., & Ding, F. (2016). "Least squares identification for Hammerstein multi-input multi-output systems based on the key-term separation technique." *Circuits, Systems, and Signal Processing,* **35**, 3745-3758.

[45] Gharehchopogh, F. S., & Gholizadeh, H. (2019). "A comprehensive survey: Whale Optimization Algorithm and its applications." *Swarm and Evolutionary Computation,* **48**, 1-24.

[46] Faris, H., Aljarah, I., Al-Betar, M. A., & Mirjalili, S. (2018). "Grey wolf optimizer: a review of recent variants and applications." *Neural computing and applications,* **30**, 413-435.

[47] Abualigah, L., Diabat, A., Mirjalili, S., Abd Elaziz, M., & Gandomi, A. H. (2021). The arithmetic optimization algorithm. Computer methods in applied mechanics and engineering, **376**, 113609.

[48] Yue, Z., & Yang, X. (2020, November). "Multi-innovation identification algorithm based on auxiliary model for Ham-

merstein output error systems." *In 2020 Chinese Automation Congress (CAC)* (pp. 5635-5640). IEEE.